Tentative identification of phase I metabolites of HU-210, a classical synthetic cannabinoid, by LC–MS/MS

Unyong Kim [a,b], Ming Ji Jin [c], Jaeick Lee [a], Sang Beom Han [b], Moon Kyo In [d], Hye Hyun Yoo [c,*]

[a] Doping Control Center, Korea Institute of Science and Technology, Seoul, South Korea
[b] Department of Pharmaceutical Analysis, College of Pharmacy, Chung-Ang University, Seoul, South Korea
[c] Department of Pharmacy, College of Pharmacy, Hanyang University, Gyeonggi-do, South Korea
[d] Drug Analysis Laboratory, Supreme Prosecutor's Office, Seoul, South Korea

ARTICLE INFO

ABSTRACT

(6aR,10aR)-9-(Hydroxymethyl)-6,6-dimethyl-3-(2-methyloctan-2-yl)-6a,7,10,10a-tetrahydrobenzo[c]chromen-1-ol (HU-210) is a synthetic cannabinoid, with a classical cannabinoid structure similar to Δ^9-tetrahydrocannabinol (Δ^9-THC). In this study, the in vitro metabolism of HU-210 was investigated in human liver microsomes to characterize associated phase I metabolites. HU-210 was incubated with human liver microsomes, and the reaction mixture was analyzed using LC–MS/MS. HU-210 was metabolized in human liver microsomes, yielding about 24 metabolites. These metabolites were structurally characterized on the basis of accurate mass analyses and MS/MS fragmentation patterns. The major metabolic route for HU-210 was oxygenation. Metabolites M1–M7 were identified as mono-oxygenated metabolites; M8–M15, mono-hydroxylated metabolites; M16–M20, di-oxygenated metabolites; and M21–M24, di-hydroxylated metabolites. These results provide evidence for in vivo HU-210 metabolism, and they may be applied to the analysis of HU-210 and its relevant metabolites in biological samples.

1. Introduction

(6aR,10aR)-9-(Hydroxymethyl)-6,6-dimethyl-3-(2-methyloctan-2-yl)-6a,7,10,10a-tetrahydrobenzo[c]chromen-1-ol (HU-210, Fig. 2), a synthetic cannabinoid, is structurally and pharmacologically similar to Δ^9-tetrahydrocannabinol (Δ^9-THC), the main active ingredient in marijuana. This compound was first synthesized from (1R,5S)-Myrtenol in 1988 [1]. Recently, it has been found in the herbal mixture "Spice", sold in the European countries [2,3]. HU-210 is a schedule I controlled substance in the United States [4].

Synthetic cannabinoids fall in a wide range of structural classes, and are mainly categorized into 2 groups: the classical structures related to THC, and the non-classical structures such as aminoalkylindole, 1,5-diarylpyrazole, quinolines, arylsulfonamides, and eicosanoids [5]. As shown in Fig. 2, HU-210 is categorized as a THC substance, and shows Δ^9-THC-like pharmacological activities [6–8]. In vitro studies show that HU-210 binds to both the brain cannabinoid receptor CB$_1$ and the peripheral cannabinoid receptor CB$_2$, with higher affinity than Δ^9-THC [9].

The metabolism of Δ^9-THC and the synthetic cannabinoid analogs such as JWH-015, JWH-018, and JWH-210 has been extensively studied by many groups [10–16]. However, to our knowledge, the chemical structures of HU-210 metabolites have not yet been elucidated. The aim of this study was to identify the phase I metabolites of HU-210 in human liver microsomes using high-resolution mass spectrometry (HR-MS) and collision-induced dissociation (CID) in MS/MS analysis.

2. Materials and methods

2.1. Chemicals and materials

HU-210 (98%) was purchased from Tocris Bioscience (Bristol, UK). HPLC-grade methanol and acetonitrile were purchased from J.T. Baker (Philipsburg, NJ, USA). β-Nicotinamide adenine dinucleotide phosphate sodium salt (β-NADP$^+$), glucose 6-phosphate, glucose-6-phosphate dehydrogenase, formic acid, KH$_2$PO$_4$, and K$_2$HPO$_4$ were obtained from Sigma–Aldrich Co. LLC (St. Louis, MO, USA). Human liver microsomes were purchased from BD Biosciences (Woburn, MA, USA). Solid-phase extraction (SPE)

* Corresponding author. Tel.: +82 31 400 5804; fax: +82 31 400 5958.
E-mail address: yoohh@hanyang.ac.kr (H.H. Yoo).

cartridge (OASIS HLB, 1 ml, 30 mg) was purchased from Waters (Milford, MA, USA). Deionized water was prepared from a Millipore Direct-Q UV system (Millipore, Milford, MA, USA). All chemicals and reagents used in this study were of analytical grade.

2.2. Biotransformation of HU-210 in human liver microsomes

HU-210 was incubated with human liver microsomes for 2 h. The 1 ml incubation mixture consisted of 1 mg protein/ml of human liver microsomes, 100 mM potassium phosphate buffer (pH 7.4), and 12.5 μg/ml HU-210. The NADPH-generating system (NGS) consisted of 1 unit of glucose-6-phosphate dehydrogenase, 0.1 M glucose-6-phosphate, and 10 mg/ml β-NADP$^+$. The reaction was started by adding NGS, and stopped by adding equal volumes of ice-cold 0.1% formic acid after a 2 h incubation period. The temperature was maintained at 37 °C during the entire incubation time.

2.3. Sample preparation

After incubation, the reaction mixtures were percolated through SPE cartridges. The SPE method involved the following steps. First, the SPE cartridge was activated with 1 ml of methanol, and equilibrated with 1 ml of deionized water. Then, the sample was loaded onto the SPE column, and the column was washed twice with 1 ml of deionized water. The reaction mixture was eluted with 1 ml of methanol, and evaporated under a stream of nitrogen at 55 °C. The residue was reconstituted with 100 μl of 70% methanol.

2.4. LC–MS/MS analysis

An LTQ-Orbitrap LC–MS/MS system (Thermo Fischer Scientific, Waltham, MA, USA) was used to identify HU-210 metabolites. The LC system was equipped with a solvent delivery pump, degasser, autosampler, and column thermostat. The separation was performed on a Hypersil Gold C$_{18}$ (150 mm × 2.1 mm, 3 μm; Thermo
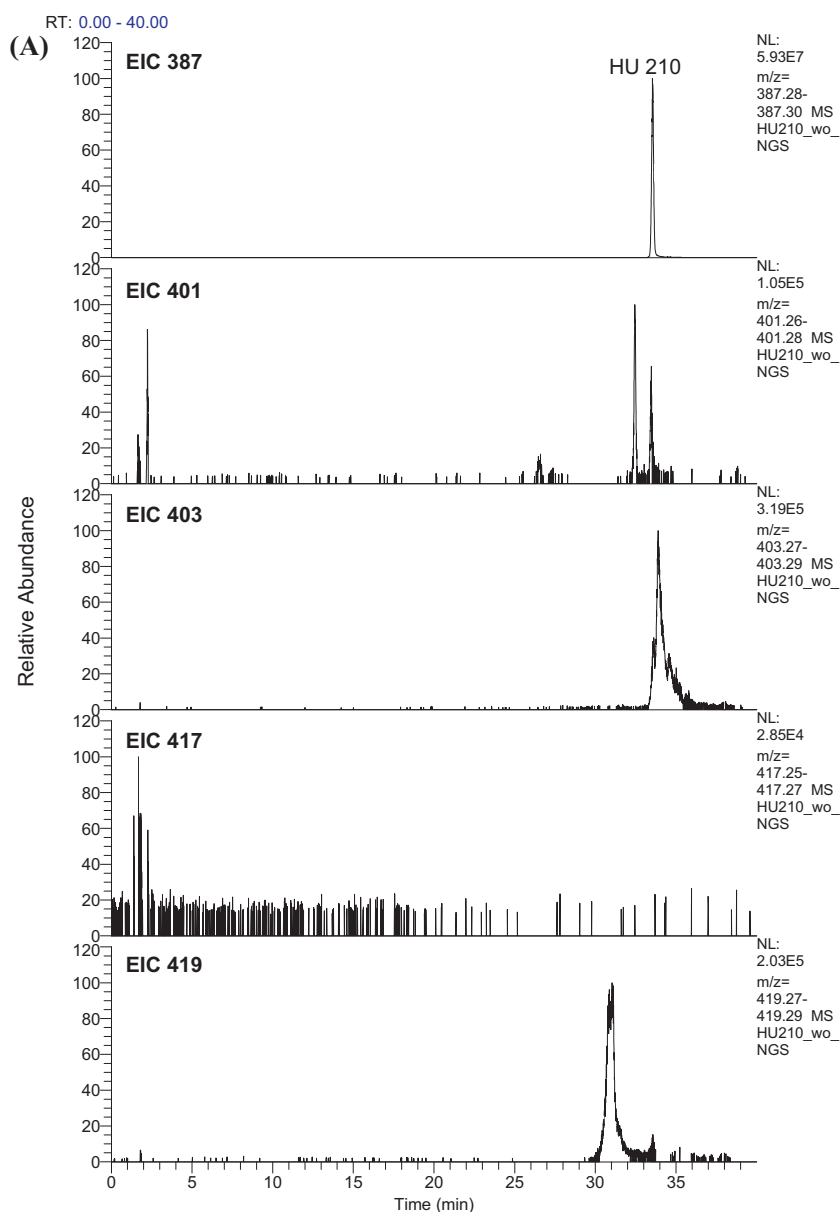

Fig. 1. Extracted ion chromatograms of HU-210 and its metabolites in human liver microsomes (A) without and (B) with NADPH.
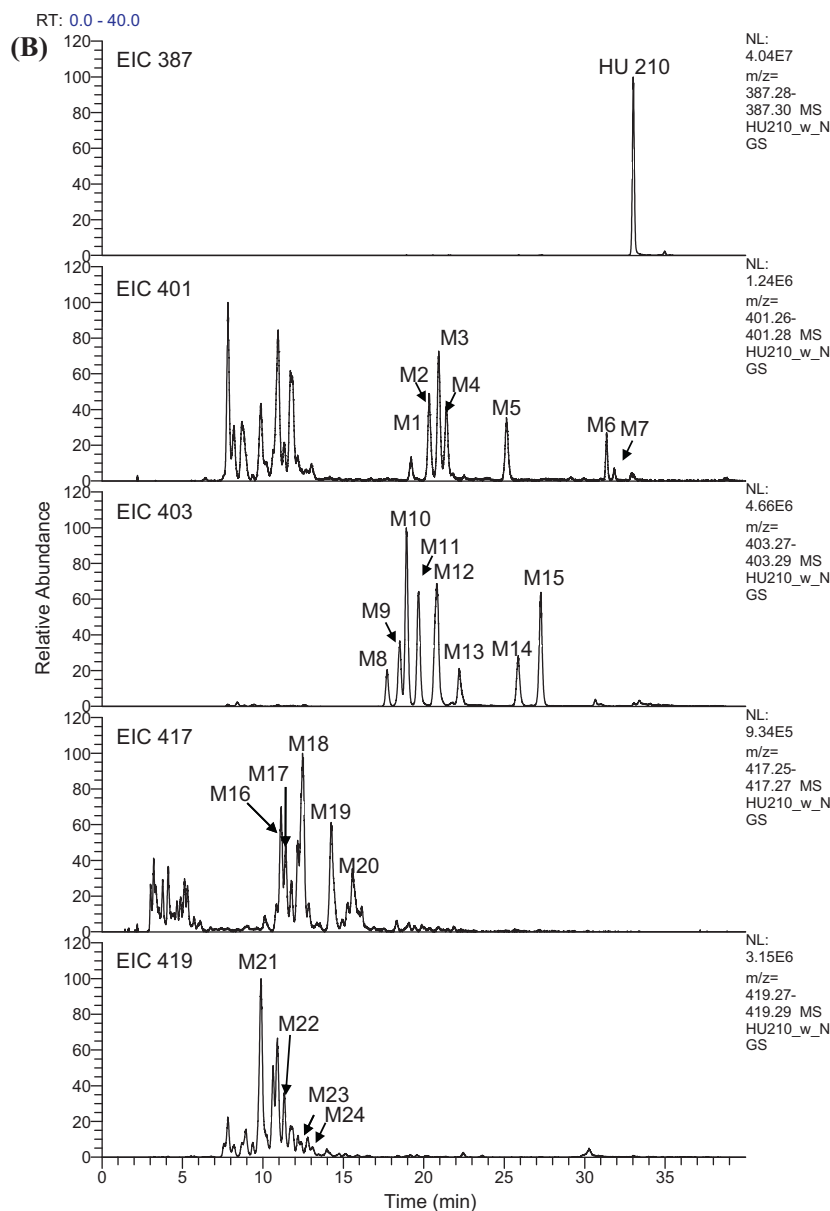
Fig. 1. *Continued* .

Fischer Scientific), using a gradient program at a flow rate of 0.2 ml/min. The mobile phase consisted of 0.1% formic acid (solvent A) and acetonitrile containing 10% of 0.1% formic acid (solvent B). The composition of solvent B was varied in the following manner: 0 min, 40%; 25 min, 70%; 29 min, 95%; 35 min, 95%; 35.1 min, 40%; and 40 min, 40%. The column thermostat was set at 35 °C for the entire analysis time. Column elutes were directly transferred to an electrospray ionization (ESI) source of LTQ-Orbitrap MS. The LTQ-Orbitrap MS was operated in the positive-ion mode, and high-resolution (Full Width Half Maximum, FWHM = 15,000) scan adopted at the mass range of m/z 100–500. The acquisition of MS^2 spectra was conducted at collision energies ranging from 20 to 25 eV for HU-210 and its suspected metabolites. The sheath gas, auxiliary gas, drying temperature, and ion spray voltage were set at 40 psi, 20 psi, 320 °C, and 4200 V, respectively.

3. Results and discussion

HU-210 was incubated with human liver microsomes (1 mg/ml), and the incubation mixture was analyzed by LC–MS and LC–MS/MS.

A representative extracted ion chromatogram (EIC) of the reaction mixture is shown in Fig. 1. A total of 24 metabolites were observed in the human liver microsomes, in the presence of NADPH. The elemental composition, retention time, and mass error to the theoretical mass of the postulated metabolites are listed in Table 1. Protonated M1–M7 were observed at m/z 401; M8–M15, m/z 403; M16–M20, m/z 417; and M21–M24, m/z 419. Therefore, we concluded that M1–M7 are oxygenated metabolites (+14 Da); M8–M15, hydroxylated metabolites (+16 Da); M16–M20, di-oxygenated metabolites (+30 Da); and M21–M24, di-hydroxylated metabolites (+32 Da). According to the elemental composition measured (Table 1), generally 1 or 2 oxygen atoms were incorporated into HU-210 by the human liver microsomal enzymes. The measured mass error between the theoretical and measured mass was less than 5 ppm for all metabolites detected. The metabolite M10 (a hydroxylated metabolite) was identified as a major metabolite in the human liver microsomes.

To elucidate the chemical structures of the proposed metabolites, the CID fragmentation of HU-210 was characterized.

Table 1
Accurate mass data for HU-210 and its proposed metabolites.

	Retention time (min)	Elemental composition ([M+H]$^+$)	Measured mass	Theoretical mass	Error (ppm)
HU 210	33.0	$C_{25}H_{39}O_3$	387.2910	387.2894	3.85
M1	19.2		401.2702		3.82
M2	20.3		401.2701		3.60
M3	20.9	C_{25}	401.2702		3.98
M4	21.4	H_{37}	401.2700	401.2686	3.29
M5	25.1	O_4	401.2701		3.52
M6	31.4		401.2701		3.52
M7	31.8		401.2698		2.84
M8	17.7		403.2859		3.90
M9	18.5		403.2862		4.88
M10	18.9		403.2862		4.80
M11	19.7	C_{25}	403.2861		4.30
M12	20.8	H_{39}	403.2860	403.2843	4.35
M13	22.2	O_4	403.2858		3.67
M14	25.9		403.2858		3.75
M15	27.3		403.2860		4.28
M16	11.2		417.2650		3.58
M17	11.4	C_{25}	417.2650		3.42
M18	12.5	H_{37}	417.2652	417.2636	3.87
M19	14.2	O_5	417.2651		3.72
M20	15.6		417.2652		4.02
M21	9.9		419.2810		4.23
M22	11.3	C_{25}	419.2808		3.87
M23	12.4	H_{39}	419.2811	419.2792	4.52
M24	13.1	O_5	419.2808		3.72

The MS^2 spectra of the protonated HU-210 and its proposed fragmentation pathways are depicted in Fig. 2. The protonated HU-210 was observed at m/z 387 ($C_{25}H_{39}O_3$), and it yielded major product ions at m/z 369 ($C_{25}H_{37}O_2$), 261 ($C_{16}H_{21}O_3$), 243 ($C_{16}H_{19}O_2$), and 201 ($C_{13}H_{13}O_2$) in MS^2 analysis. The MS^2 product ions at m/z 369 were generated by the loss of 1 H_2O molecule (−18 Da) probably from the methylcyclohexene ring (ring A) with a rearrangement of the double bond. The product ion at m/z 261 was formed via the release of an alkyl side chain from the phenol ring. The fragment ion at m/z 243 was produced by a loss of 1 H_2O molecule from the ion at m/z 261. The fragment ions observed at m/z 201 were formed via the release of an isopropyl group (−C_3H_6, −42 Da) from the fragment ion at m/z 243. These ions were used as key elements to determine modified sites in the structures of HU-210 metabolites. It is interesting that

the ion-trap CID fragmentation pattern of HU-210 appears to be different from that in triple-quadrupole or quadrupole-time-of-flight (Q-TOF) MS. In case of THC, a structural analog of HU-210, the product ion resulting from an alkyl side chain was less abundant but rather cleavage and rearrangement of the methylcyclohexene ring or cleavage of the ring B were the major fragmentation pathways in triple-quadrupole MS [17]. With Q-TOF MS, the pattern seems to be somewhat similar to that in the ion-trap MS but a loss of the alkyl side chain was still not predominantly observed [18].

The structure of each metabolite was characterized on the basis of MS analysis and fragmentation patterns of HU-210. M1, M2, M3, M4, M5, M6, and M7 were observed at 19.2, 20.3, 20.9, 21.4, 25.1, 31.4, and 31.8 min, respectively, with protonated molecules at m/z 401 ($C_{25}H_{37}O_4$). The molecular weights of M1, M2, M3, M4, M5,
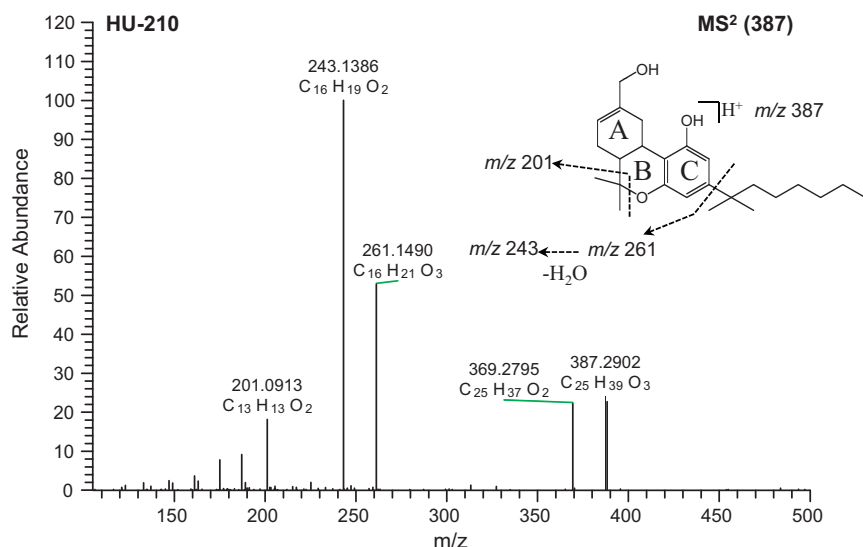
Fig. 2. Product ion mass spectrum of HU-210.

M6, and M7 were 14 Da higher than that of HU-210 ($C_{25}H_{39}O_3$). The MS^2 spectra of M1–M5 showed major product ions at m/z 383 ($C_{25}H_{35}O_3$), m/z 365 ($C_{25}H_{33}O_2$), m/z 341 ($C_{22}H_{29}O_3$), and m/z 243 ($C_{16}H_{19}O_2$) (Fig. 3A). The product ions at m/z 383 and 365 resulted from the sequential dehydration of the precursor ion at m/z 401; the ion at m/z 341 was generated by a loss of C_3H_6 (−42 Da) from the ion at m/z 383, and a similar fragmentation pattern was observed in the parent compound (m/z 243 → m/z 201). The ion at m/z 243 was identical to the product ion of HU-210. Thus, M1–M5 were assigned as metabolites that were mono-oxygenated in the alkyl side chain of the phenol ring. M6 and M7 yielded major product ions at m/z 383 ($C_{25}H_{35}O_3$), m/z 341 ($C_{22}H_{29}O_3$), m/z 275 ($C_{16}H_{19}O_4$), and m/z 257 ($C_{16}H_{17}O_3$) (Fig. 3B). The product ion at m/z 383 resulted from the dehydration of the protonated molecule. The product ion at m/z 341 was generated by a loss of C_3H_6 (−42 Da) from the ion at m/z 383 as observed in M1–M5. The product ions at m/z 275 and 257 showed 14 Da higher m/z values than those of HU-210 at m/z 261 and m/z 243. Accordingly, it is believed that the oxygenations may occur at ring A or its associated parts. The order of fragmentation, *i.e.*, first alkyl chain, then the ring B, or the reverse, may depend on the biotransformation position. As for HU-210, the fragmentation of the side alkyl chain occurred prior to the cleavage of the ring B (m/z 243 > m/z 201) whereas in M1–M5, the cleavage of the ring B priorly occurred (m/z 383 > m/z 341). This reveals that the modification in the alkyl side chain altered the fragmentation pattern of M1–M5.
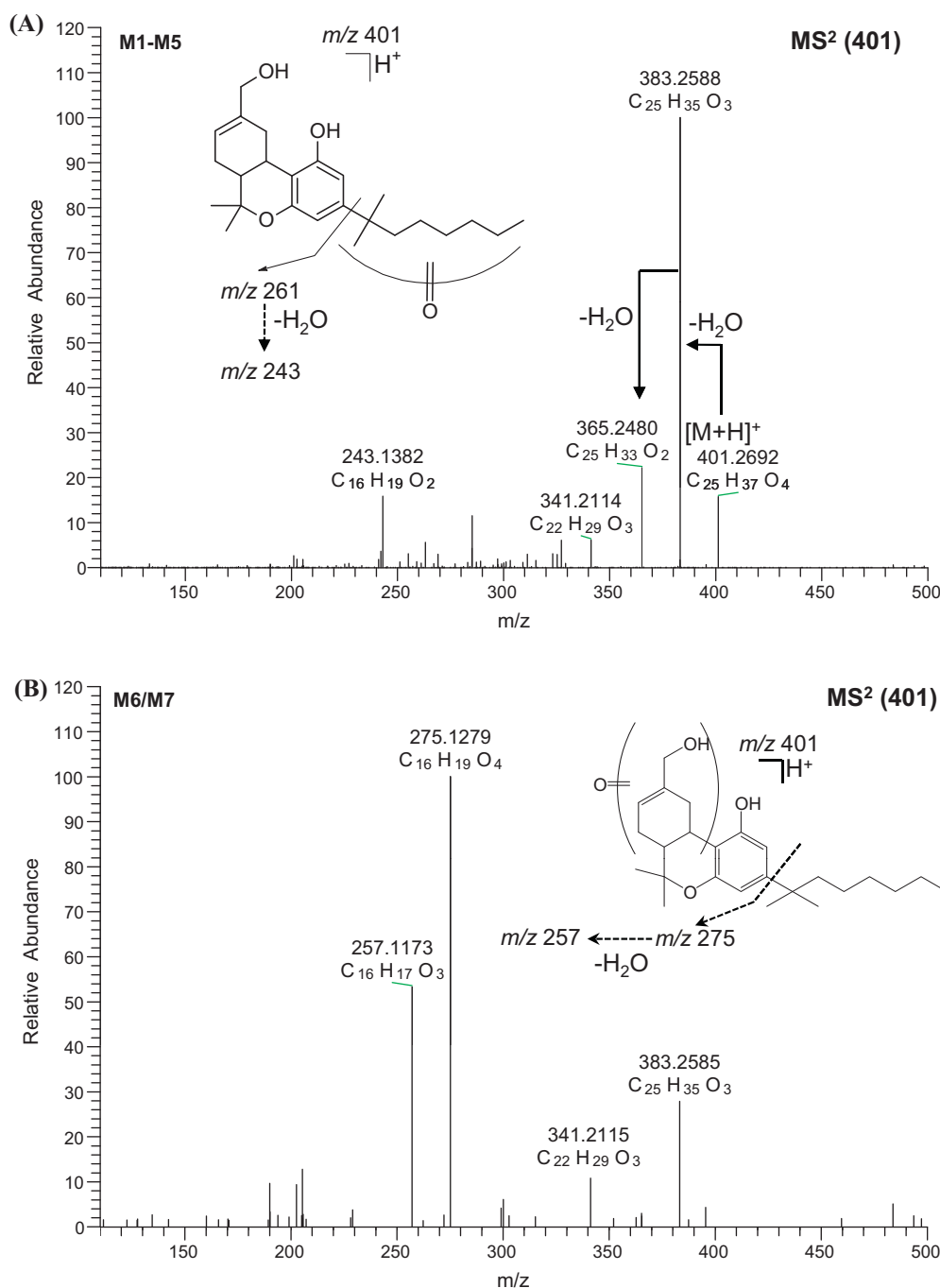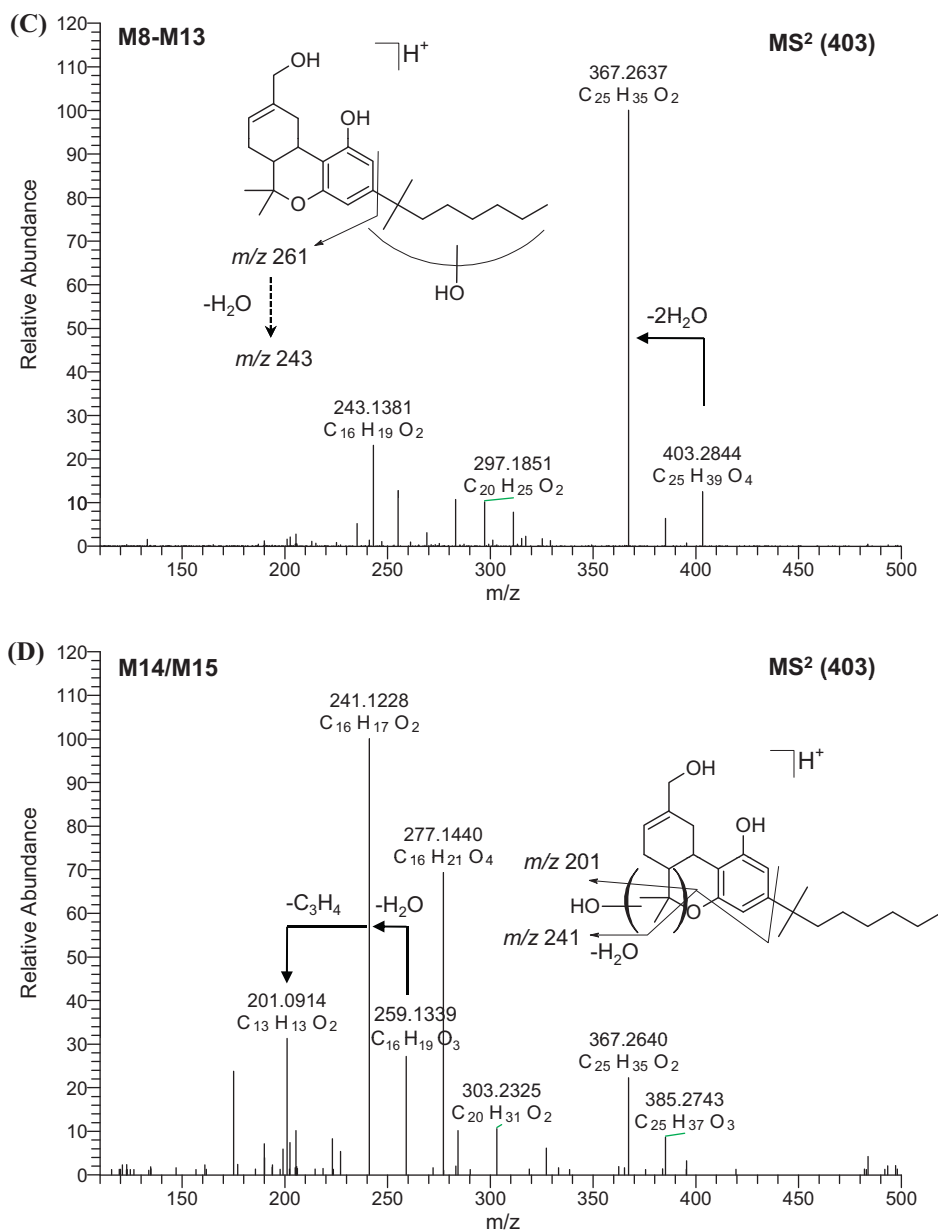

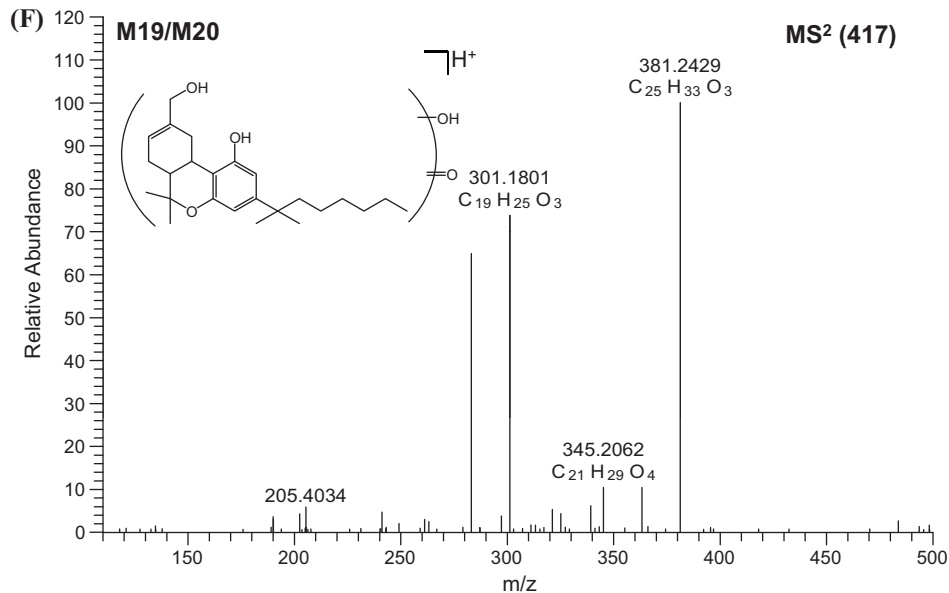**Fig. 3.** Product ion mass spectra of the proposed metabolites of HU-210.
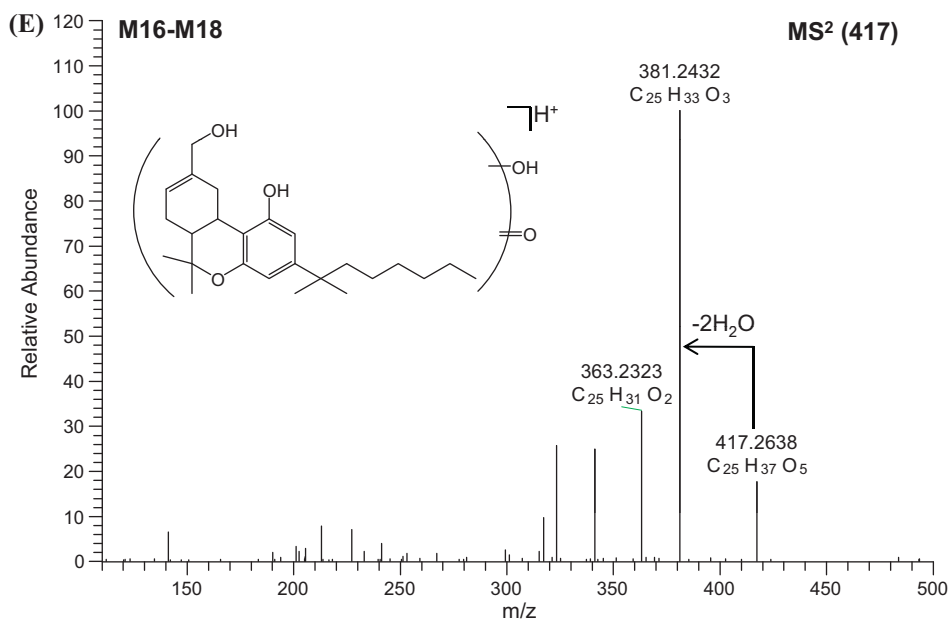
Continued.

M8, M9, M10, M11, M12, M13, M14, and M15 were observed at 17.7, 18.5, 18.9, 19.7, 20.8, 22.2, 25.9, and 27.3 min, respectively, with protonated molecules at m/z 403 ($C_{25}H_{39}O_4$). The associated m/z value was 16 Da higher than that of HU-210; therefore, all these were considered mono-hydroxylated metabolites. The MS^2 spectrum of M8–M13 showed major product ions at m/z 367 ($C_{25}H_{35}O_2$), 297 ($C_{20}H_{25}O_2$), and 243 ($C_{16}H_{19}O_2$) (Fig. 3C). The ion at m/z 367 was generated by the loss of 2 H_2O molecules (-36 Da). The ion at m/z 297 was generated by the loss of a hydroxypentyl group ($-C_5H_{11}OH$, -88 Da) possibly from the ion at m/z 385. The ion at m/z 243 was the common fragment ion observed for the parent compound and M1–M5. The presence of the product ion at m/z 243 indicates that the site of hydroxylation may be at the alkyl side chain of the phenol ring. M14 and M15 yielded major product ions at m/z 385 ($C_{25}H_{37}O_3$), 367 ($C_{25}H_{35}O_2$), 277 ($C_{16}H_{21}O_4$), 259 ($C_{16}H_{19}O_3$), 241 ($C_{16}H_{17}O_2$), and 201 ($C_{13}H_{13}O_2$) (Fig. 3D). The product ions at m/z 385 and 367 resulted from a sequential loss of 2 H_2O molecules. The ions at m/z 277 and 259 were 16 Da higher than the corresponding fragment ions of HU-210.

The product ion at m/z 201 was also found in the MS^2 spectrum of HU-210. These results collectively suggest that the site of hydroxylation is considered to be the di-methyl groups of the ring B.

M16, M17, M18, M19, and M20 were observed at 11.2, 11.4, 12.5, 14.2, and 15.6 min, respectively, with protonated molecules at m/z 417 ($C_{25}H_{37}O_5$), which was 30 Da higher than that of HU-210, and therefore, they were believed to be di-oxygenated metabolites. The MS^2 spectrum of M16–M18 showed major product ions at m/z 381 ($C_{25}H_{33}O_3$) and m/z 363 ($C_{25}H_{31}O_2$), through a sequential loss of 3 and 2 H_2O molecules, respectively (Fig. 3E). Other fragment ions with patterns similar to those of the parent compound or other metabolites were also observed. The MS^2 spectrum of M19 and M20 (Fig. 3F) was slightly different from that of M16–M18; the ions at m/z 381 of ($C_{25}H_{33}O_3$) and m/z 301 ($C_{19}H_{25}O_3$) were the major product ions. The product ion at m/z 301 resulted from the loss of $C_6H_{12}O_2$ via cleavage at the branched site of the alkyl side chain. This reveals that the metabolic change(s) occurred in the right side of the branch of the alkyl chain. However, the metabolic sites where

(E) M16-M18 MS² (417)

381.2432 $C_{25}H_{33}O_3$

363.2323 $C_{25}H_{31}O_2$

417.2638 $C_{25}H_{37}O_5$

-2H₂O

(F) M19/M20 MS² (417)

381.2429 $C_{25}H_{33}O_3$

301.1801 $C_{19}H_{25}O_3$

345.2062 $C_{21}H_{29}O_4$

205.4034

Continued.

2 oxygen atoms were introduced could not be assigned on the basis of only the MS data.

M21, M22, M23, and M24 were observed at 9.9, 11.3, 12.4, and 13.1 min, respectively, with protonated molecules at m/z 419 ($C_{25}H_{39}O_5$). The associated m/z values were 32 Da higher than that of HU-210, and thus, they were considered as di-hydroxylated metabolites. The MS² spectrum showed major product ions at m/z 401 ($C_{25}H_{35}O_3$), m/z 383 ($C_{25}H_{35}O_3$), m/z 365 ($C_{25}H_{33}O_2$), m/z 285 ($C_{18}H_{21}O_3$), m/z 277 ($C_{16}H_{21}O_4$), and m/z 241 ($C_{16}H_{17}O_2$) (Fig. 3G). The ions at m/z 401, 383, and 365, were formed by a sequential loss of 3 H_2O molecules. The ion at m/z 277 was 16 Da higher than that of HU-210 at m/z 261. This indicates that at least 1 hydroxyl group exists in ring A, B, or C, and another hydroxyl group may, therefore, be located in the alkyl side chain.

In the present study, the metabolic sites of individual metabolites could not be assigned due to the limitation of LC–MS/MS analysis based on CID fragmentation patterns but groups of metabolites have been identified. NMR studies will be necessary for complete structural characterization of the individual metabolites. With regard to the relative amount of each metabolite, present work is not a quantitative study and only very cautious conclusions should be drawn from the relative peak areas in the figures due to the possible differences on the electrospray ionization MS responses.

Synthetic cannabinoids are mainly classified into three structural types: classical cannabinoids (HU-210), naphthoylindole analogs (JWH-018), and phenylcyclohexyl analogs (CP 47, 497). Among them, the JWH-018 type-cannabinoids have been investigated most extensively with regard to detection methods or metabolic pathways and the associated metabolites are reportedly metabolized *via* phase I metabolic reactions such as hydroxylation, dehydration, dihydrodiol formation, N-dealkylation, and carboxylation [11,12,19–21]. The alkyl side chain is one of the major metabolic sites for hydroxylation or dehydration. During *in vivo* metabolism, JWH-018 is initially metabolized to yield mono-hydroxylated metabolites, and further metabolized to form

Continued.
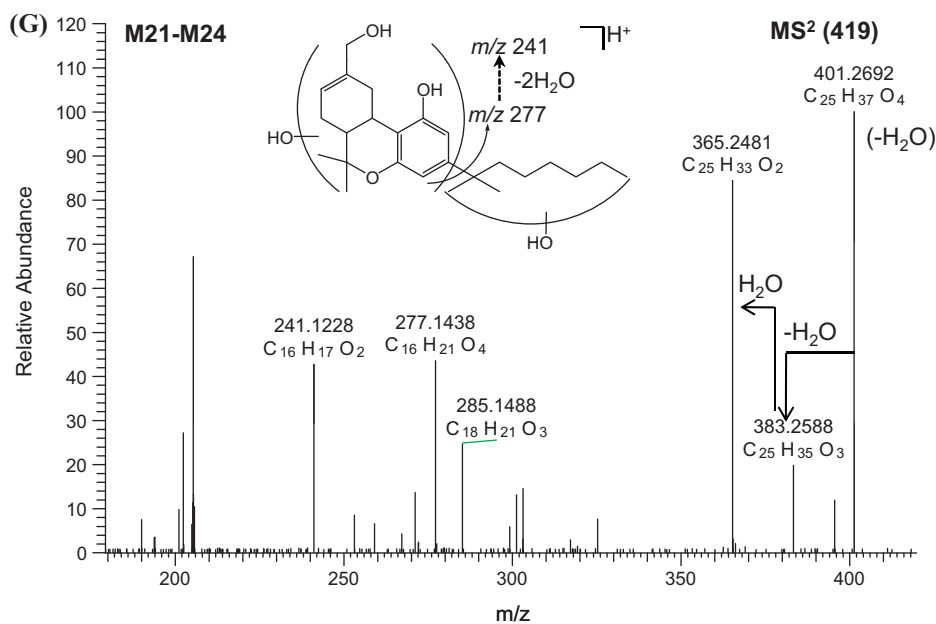
glucuronide conjugates, which are subsequently excreted into urine. In the case of CP 47,497, hydroxylation at the alkyl side chain was observed as a major metabolic pathway for phase I metabolism (data not published). HU-210 showed a similar metabolic pattern with other synthetic cannabinoids, in particular, CP 47,497; the major metabolic pathway is hydroxylation or oxygenation. However, in this study, HU-210 was found to be more extensively metabolized in human liver microsomes compared to CP 47,497. Compared with the metabolism of THC, the major metabolites of THC are carboxy and hydroxyl metabolites and the methyl moiety of the cyclohexene is the main metabolic site but this did not pertain to HU-210 due to the structural modification of the methyl cyclohexene ring [17,18].

4. Conclusion

The *in vitro* metabolism of HU-210 was characterized based on accurate mass analysis and CID fragmentation pattern using LC–MS/MS. HU-210 was metabolized to yield a total of 24 metabolites in human liver microsomes. The major metabolic route of HU-210 was oxygenation. To our knowledge, this is the first report on the metabolic profiling of HU-210 in human liver microsomes. These results can provide evidence for *in vivo* metabolism of HU-210 and be applied to analysis of HU-210 and its relevant metabolites in biological samples.

References

[1] R. Mechoulam, N. Lander, A. Breuer, J. Zahalka, Synthesis of the individual, pharmacologically distinct, enantiomers of a tetrahydrocannabinol derivative, Tetrahedron: Asymmetry 1 (1990) 315–318.
[2] N. Uchiyama, R. Kikura-Hanajiri, J. Ogata, Y. Goda, Chemical analysis of synthetic cannabinoids as designer drugs in herbal products, Forensic Sci. Int. 198 (2010) 31–38.
[3] V. Auwärter, S. Dresen, W. Weinmann, M. Müller, M. Pütz, N. Ferreirós, 'Spice' and other herbal blends: harmless incense or cannabinoid designer drugs? J. Mass. Spectrom. 44 (2009) 832–837.
[4] HU-210 [(6aR,10aR)-9-(hydroxymethyl)-6,6-dimethyl-3-(2-methyloctan-2-yl)-6a,7,10,10a-tetrahydrobenzo[c] chromen-1-ol] [Purported Ingredient of "Spice"], U.S. Department of Justice Drug Enforcement Administration Office of Diversion Control, 2009.
[5] D.M. Lambert, C.J. Fowler, The endocannabinoid system: drug targets, lead compounds, and potential therapeutic applications, J. Med. Chem. 48 (2005) 5059–5087.
[6] H. Ovadia, A. Wohlman, R. Mechoulam, J. Weidenfeld, Characterization of the hypothermic effect of the synthetic cannabinoid HU-210 in the rat. Relation to the adrenergic system and endogenous pyrogens, Neuropharmacology 34 (1995) 175–180.
[7] P.J. Little, D.R. Compton, R. Mechoulam, B.R. Martin, Stereochemical effects of 11-OH-[Delta]8-THC-dimethylheptyl in mice and dogs, Pharmacol. Biochem. Behav. 32 (1989) 661–666.
[8] D. Giuliani, F. Ferrari, A. Ottani, The cannabinoid agonist HU 210 modifies rat behavioural responses to novelty and stress, Pharmacol. Res. 41 (2000) 45–51.
[9] A. Ottani, D. Giuliani, HU 210: a potent tool for investigations of the cannabinoid system, CNS Drug Rev. 7 (2001) 131–145.
[10] Q. Zhang, P. Ma, R.B. Cole, G. Wang, Identification of in vitro metabolites of JWH-015, an aminoalkylindole agonist for the peripheral cannabinoid receptor (CB2) by HPLC–MS/MS, Anal. Bioanal. Chem. 386 (2006) 1345–1355.
[11] T. Sobolevsky, I. Prasolov, G. Rodchenkov, Detection of JWH-018 metabolites in smoking mixture post-administration urine, Forensic Sci. Int. 200 (2010) 141–147.
[12] I. Möller, A. Wintermeyer, K. Bender, M. Jübner, A. Thomas, O. Krug, W. Schänzer, M. Thevis, Screening for the synthetic cannabinoid JWH-018 and its major metabolites in human doping controls, Drug Test. Anal. 3 (2011) 609–620.
[13] E.G. Leighty, Metabolism and distribution of cannabinoids in rats after different methods of administration, Biochem. Pharmacol. 22 (1973) 1613–1621.
[14] D.J. Harvey, N.K. Brown, Comparative in vitro metabolism of the cannabinoids, Pharmacol. Biochem. Behav. 40 (1991) 533–540.
[15] B. Maralikova, W. Weinmann, Simultaneous determination of Δ9-tetrahydrocannabinol, 11-hydroxy-Δ9-tetrahydrocannabinol and 11-nor-9-carboxy-Δ9-tetrahydrocannabinol in human plasma by high-performance liquid chromatography/tandem mass spectrometry, J. Mass Spectrom. 39 (2004) 526–531.
[16] J. Jung, M.R. Meyer, H.H. Maurer, C. Neusüß, W. Weinmann, V. Auwärter, Studies on the metabolism of the Δ9-tetrahydrocannabinol precursor Δ9-tetrahydrocannabinolic acid A (Δ9-THCA-A) in rat using LC–MS/MS, LC-QTOF MS and GC–MS techniques, J. Mass Spectrom. 44 (2009) 1423–1433.
[17] B. Maralikova, W. Weinmann, Simultaneous determination of Delta9-tetrahydrocannabinol, 11-hydroxy-Delta9-tetrahydrocannabinol and 11-nor-9-carboxy-Delta9-tetrahydrocannabinol in human plasma by high-performance liquid chromatography/tandem mass spectrometry, J. Mass Spectrom. 39 (2004) 526–531.
[18] L. Bijlsma, J.V. Sancho, F. Hernández, W.M. Niessen, Fragmentation pathways of drugs of abuse and their metabolites based on QTOF MS/MS and MS(E) accurate-mass spectra, J. Mass Spectrom. 46 (2011) 865–875.

[19] A. Wintermeyer, I. Möller, M. Thevis, M. Jübner, J. Beike, M.A. Rothschild, K. Bender, In vitro phase I metabolism of the synthetic cannabimimetic JWH-018, Anal. Bioanal. Chem. 398 (2010) 2141–2153.

[20] C.L. Moran, V.H. Le, K.C. Chimalakonda, A.L. Smedley, F.D. Lackey, S.N. Owen, P.D. Kennedy, G.W. Endres, F.L. Ciske, J.B. Kramer, A.M. Kornilov, L.D. Bratton, P.J. Dobrowolski, W.D. Wessinger, W.E. Fantegrossi, P.L. Prather, L.P. James, A. Radominska-Pandya, J.H. Moran, Quantitative measurement of JWH-018 and JWH-073 metabolites excreted in human urine, Anal. Chem. 83 (2011) 4228–4236.

[21] A. Grigoryev, S. Savchuk, A. Melnik, N. Moskaleva, J. Dzhurko, M. Ershov, A. Nosyrev, A. Vedenin, B. Izotov, I. Zabirova, V. Rozhanets, Chromatography–mass spectrometry studies on the metabolism of synthetic cannabinoids JWH-018 and JWH-073, psychoactive components of smoking mixtures, J. Chromatogr. B: Analyt. Technol. Biomed. Life Sci. 879 (2011) 1126–1136.